MOLECULAR-ION ELECTROGASDYNAMIC FLOW CHANNEL

by

David William Wallace

United States Naval Postgraduate School

THESIS

MOLECULAR-ION ELECTROGASDYNAMIC

FLOW CHANNEL

by

David William Wallace

June 1969

Molecular-ion Electrogasdynamic Flow Channel

by

David William Wallace
Lieutenant (junior grade), United States Navy
B. S., United States Naval Academy, 1968

Submitted in partial fulfillment of the
requirements for the degree of

MASTER OF SCIENCE

IN

AERONAUTICAL ENGINEERING

from the

NAVAL POSTGRADUATE SCHOOL
June 1969

ABSTRACT

This investigation evaluates the operating characteristics of an EGD (electrogasdynamic) generator system which utilizes air both as the carrier fluid and as the source of injected ions. The design and construction of a flow channel and a corona ion injector are discussed, the performance of the ion injector is examined, and the results of attempts to obtain work by EGD energy conversion are presented. The experimental results presented and discussed are in reasonable agreement with expectations. The high mobility of molecular ions inhibits the conversion process and only 0.5% of the ions were removed from the corona by the air flow. Suggestions for improvements on the present system and the design of an advanced system are made.

TABLE OF CONTENTS

LIST OF ILLUSTRATIONS

LIST OF SYMBOLS

Symbol	
A'	Percent of test channel cross-section within boundary layer
b	Barometric pressure (in. Hg.)
D_2	Orifice diameter (inches)
h_w	Pressure differential across the orifice (in. H_2O)
I_c	Corona current
I_g	Collector current
K	Dimensionless discharge coefficient
KV	Kilovolt (10^3 volts)
M	Mach number
P_b	Absolute pressure at test section (psi)
P_1	Absolute pressure at orifice (psi)
ΔP	Pressure differential of pitot-static tube (cm H_2O)
q	Rate of heat loss
RMS	Root-mean-square
T	Temperature (°R)
T_f	Flow field temperature
T_w	Wire temperature
U_∞	Freestream velocity (ft/sec)
u	Average velocity in the boundary layer (ft/sec)
$\bar{u}$	Mass-mean velocity (ft/sec)

V_c	Corona voltage
Y_1	Dimensionless expansion factor
α	Dimensionless area multiplier
ρ_b	Fluid density at test channel (lb/ft^3)
ρ_1	Fluid density at orifice (lb/ft^3)
μA	Micro-ampere (10^{-6} amp)

ACKNOWLEDGEMENT

The author expresses his sincere appreciation to Professor Oscar Biblarz of the Naval Postgraduate School, Monterey, California, for his assistance and guidance, and to Mr. Pat Hickey, Naval Postgraduate School technician, for his many technical services. Special thanks are given to fellow student W. T. Ober, LT(j.g.), USN, for principally providing the corona ion injector.

I. INTRODUCTION

High voltage, low current power sources have not been exploited commercially due to their high cost and the generally bulky size of the necessary equipment. The most familiar apparatus of this type is the Van de Graaff generator which 'pumps' charges from ground to a collector device by means of a moving belt, thereby generating a high electric potential between the collector and ground. In 1959, W. E. Bennett[1] pointed out that since a greater charge could be carried in a volume than on a surface (such as the belt of a Van de Graaff generator) and since the charge transfer rate could be much higher with a moving fluid flow, the fluidic Van de Graaff generator promised higher currents and greater efficiency. Such a device is variously termed an electrogasdynamic (EGD), electrohydrodynamic (EHD), or electrofluiddynamic (EFD) generator, depending on the transport medium used, and is the subject of this investigation.

As indicated by the title of this report, we have chosen to pursue the investigation of the electrogasdynamic type device, henceforth referred to as the EGD system. Although it has been shown by various researchers[3] that higher efficiencies and greater currents are obtained if micron-sized charged particles are injected into the system, we have confined ourselves in this project to molecular ions, using air both as the transport fluid and the source of charged particles. It should

be noted that this investigation is the preliminary stage of a more comprehensive, long-term project being carried on by Professor Oscar Biblarz, Department of Aeronautics, Naval Postgraduate School.

An experimental EGD generator system was fabricated and installed in Building 230 at the Naval Postgraduate School, Monterey, California, utilizing a corona discharge to provide charged particles. A test program was carried out to determine the basic performance of the flow channel and ion injector, and to evaluate the molecular-ion EGD generator system as a whole.

II. PRINCIPLES OF OPERATION

The electrogasdynamic generator is analogous to the Van de Graaff generator in principle: a moving medium transports charged particles against an electric field to a collector. Thus the kinetic energy of the transport medium is converted into electrical energy. In the case of the Van de Graaff generator, a moving belt is used to transport the charged particles. For the Van de Graaff generator, the amount of charge transported is limited by two physical criteria --- the surface area of the belt and the velocity of the belt. By using a moving fluid for the transport medium, the amount of charge transportable is greatly increased because: 1) the amount of charge carried is now more a function of volume rather than surface area; and 2) the fluid can travel at a higher speed than a mechanical belt.[2]

An EGD generator consists of three basic components: 1) a charged-particle injector; 2) a dielectric conversion section; 3) a collector. Figure 1 is a schematic of an EGD generator system.

Charged particle injection at near-atmospheric pressures is most easily accomplished using a corona discharge[4]. A high voltage is placed across a needle and ring, producing an intense electrical field in the region between the needle and the ring. Ionization of gas molecules in this region is caused by the electric field, with a sheath of oppositely charged particles being formed around the needle. This charge sheath intensifies the field adjacent to the needle, and diminishes

the field external to the sheath extending to the ring. Ions of like charge to the needle then drift toward the ring, as shown in Figure 2. The ionization process is exponential in nature, and produces electron avalanches which are a mechanism by which current flows across the corona gap. Each avalanch decreases the gap potential. Thus at low voltages, complete ionization across the gap is stopped by the associated potential decrease before breakdown can occur. At a sufficiently high voltage, however, the gap potential, even with the loss due to the electron avalanches, is sufficient to cause complete ionization and a direct current flow across the gap. Breakdown is undesireable because ions are no longer drifting alone towards the ring.[5]

In the case of a positive needle corona, gas molecules are stripped of an electron and drift towards the ring as positive charged particles. With a negative needle corona, the drifting particles may be free electrons or negative ions formed by electron attachment. Since both free electrons and negative ions have a higher mobility than positive ions, a negative needle corona produces higher current than a positive needle corona. As long as the breakdown potential of the gas is not exceeded, any current flowing through the corona unit will be due to ions reaching the ring and being neutralized. Ideally, if an external force could be applied which would remove all the charged particles drifting toward the ring before they reached it, thus preventing current flow across the corona, the net work done by the corona circuit power source would be zero.

The external force used to remove the charged particles from the corona field may be derived from the kinetic energy of a gas flow. For the ions drifting toward the ring to be removed by the air flow, the kinetic energy imparted to them by the flow must be greater than the electrostatic energy of the corona unit. In the case of molecular-sized particles this transfer of kinetic energy is accomplished by molecular collisions between the air flow particles and the charged ions, and thus is dependent on the mobility of the charged particles. (Mobility is defined as the average drift velocity per unit electric field, where the average drift velocity is related to the reduction of the ion mean free path by collisions with the gas molecules). Mobility decreases as density increases, and therefore is also inversely related to pressure. Thus the removal of charged particles from the corona, which increases as mobility decreases, increases with the increasing pressure.

Once the gas molecules, now charged, are removed from the corona, their electrical energy is retrieved by means of a collector. This may be a wire mesh, a hollow cylinder, or a conducting rod. The rod seems to be the most efficient method of collection, although it is not understood exactly how the collection process occurs.[6]

The retrieval of charges at the collector causes a buildup of a potential between the collector and ground, and the resulting current flow through the collector circuit is the work done by the air flow, or the output of the EGD system.

Figure 3 shows the wiring circuit of an EGD system. Ideally, there will be no current flow through the corona circuit ($I_C = 0$) since the ions will be swept downstream to the collector, producing a collector current (I_G).

With the corona-conversion process acting as a generator, a typical load curve might be obtained by placing the generator output across a suitable variable resistance. For a given resistance, a voltage versus current curve could be obtained which would include the maximum voltage-no current case (open circuit) and the no voltage-maximum current case (short circuit) as its limits. Since the conversion process at the corona was of primary interest, e.g., the percentage of corona ions being forced to the collector, the short circuit setup which indicated largest current through the collector was first used. After a significant collector current had been detected, the generator performance would have been further evaluated by determining the entire load curve, had more time been available.

III. EXPERIMENTAL APPARATUS

The EGD system fabricated was designed for approximate flow speeds of Mach 0.3 and for minimum flow turbulence at the test section where the corona unit was placed. Figure 4 shows the system schematic, while Figure 5 shows the flow channel in detail. A photograph and engineering drawing of the flow channel are provided in Figures 6 and 7, respectively. Air was supplied by a Carrier three stage centrifugal compressor (Figure 8) with a 4000 ft^3/min. maximum inlet capacity and a maximum pressure ratio of two. The exit air temperature varied from 65°F to 240°F. The flow could be regulated, as shown in Figure 4, by two valves and exhausted to the atmosphere. The flow orifice shown in Figure 4 was used only to determine the accuracy of the pitot-static tube located in the flow channel, which in conjunction with the manometer bank was used to determine the flow rate setting (See Appendix A). The cooling bank was used to keep the temperature of the air flow close to ambient and to hasten the temperature stabilization. An iron-constantan thermocouple was used to determine the flow temperature.

The test channel was made of three-eighths inch Plexiglass which was chosen because of its high dielectric properties (volume resistivity=10^{12} ohms-cm). In addition, Plexiglass permitted the investigator to observe the interior of the test channel. A test channel plenum to test section area ratio of 10 to 1, and a series of consecutively finer honeycomb and wire mesh were used to reduce the freestream flow

turbulence to a level comparable to contemporary flow channels--0.14% RMS (i.e., the time-averaged magnitude of velocity fluctuations was 0.14% of the freestream velocity) according to a Ballantine RMS voltmeter. Using a Security Associates single-channel hot-wire probe, the channel boundary layers were determined so that the corona unit might be placed outside of the boundary layers. The boundary layers were found to be not fully developed, and at most only 0.15 inch thick which presented no interference with the test region.

Because the efficiency of a corona discharge depends in part on pressure, being more efficient at lower pressures, the corona unit was mounted on the downstream side of a Plexiglass cylinder placed horizontally in the flow channel. Thus, due to the pressure drop downstream of the cylinder, the pressure at the needle where the corona action is strongest was relatively low compared to the pressure at the ring, where the conversion process occurs. It was observed that the corona performance was also affected by turbulence in that turbulence tended to inhibit breakdown. Although this aspect of the corona unit was not investigated, turbulence levels in the wake of the cylinder were determined, and are given in Figure 9. The ring and needle leads were buried in the Plexiglass to minimize the possibility of point discharges and subsequent current leaks. Figure 10 is an isometric of the corona unit, while Figure 11 provides an engineering drawing of the corona device. The cylinder was three-eighths inch in diameter. The Reynolds number based on freestream velocity and cylinder diameter

for M=0.3 was 6.63×10^4, which is subcritical, indicating separation close to 90° from the horizontal centerline. The needle and ring were made of pure platinum wire with wire sizes of 0.010 and 0.020 inches respectively. Three different corona configurations were used. Their pertinent dimensions are summarized as follows:

Ring	Needle Length	Distance From Cylinder to Ring (smallest)	Ring Diameter
1	0.187 inch	0.187 inch	0.394 inch
2	0.062 inch	0.187 inch	0.315 inch
3	0.187 inch	0.187 inch	0.750 inch

The collector unit consisted of an iron rod (1/8" Dia.), sharpened to a needle point, which was mounted on an insulated traversal unit allowing vertical and horizontal movement for any axial position.

High voltage power was supplied to the corona unit by a Sorensen High Voltage D.C. Power Supply. This power supply produces up to 30KV and 20MA of current with a ripple of 2%, and has trip controls for both voltage and current. It also has the feature of reversible polarity.

The high voltage across the corona was measured with a Sensitive Research electrostatic voltmeter. This instrument has an internal impedance of 5×10^{15} ohms and reads RMS voltages up to 40KV on four scales.

Corona currents were measured with a Simpson 0-100 μA ammeter.

Collector currents were read using a Calico Digital Multimeter which had an amperage range of 0.01-1000 μA through the use of various scales.

Figure 12 is a photograph of the experimental setup.

IV. EXPERIMENTAL PROCEDURE

This investigation was divided into two parts: 1) design and construction of apparatus and determination of its airflow properties, and 2) testing of the EGD system.

The first part was preliminary to the second and consisted of determining and reducing, if necessary, the freestream turbulence; determining the test channel wall boundary layers; and exploring the corona-cylinder wake (See Appendix B). Turbulence levels were determined using the RMS voltmeter in conjunction with the hot-wire anemometer, assuming the boundary layer to start where the velocity dropped to 0.99 of the freestream velocity. After the freestream turbulence was lowered to an acceptable level by means of honeycomb and wire mesh screen, and the boundary layers were determined, the corona cylinder was placed in the test channel. Turbulence levels and wake boundaries were determined in order to insure that the corona ring was placed within the wake region where high turbulence levels would inhibit breakdown. This completed preliminary work and actual testing of the corona unit was begun.

The corona unit was first tested for continuity of all electrical connections. An effort was then made to minimize point sources which might enable current leakage. This problem was primarily attacked by devising the brass connector spheres shown in Figure 13. Then data for corona curves was taken without air flow, followed by data for

corona curves with air flow. Curves were obtained by holding the flow velocity constant and varying corona voltage, and by keeping corona voltage constant and varying flow velocity. Finally, the collector unit was positioned downstream of the corona unit. If a collector current was detected, the unit was moved about to determine the effect of position on collector current. Prior to each test run, the corona unit was cleansed with freon. This procedure was carried out for each of the three corona units.

V. RESULTS AND CONCLUSIONS

Figures 14 thru 17 show the data obtained by the procedure outlined previously. The general pattern is the same for each corona configuration (see page 19, this report), and thus only curves for a single configuration are given. Data reproductability was generally good. The main cause of data error was improper circuit connection; specifically, if the contact screws were not seated properly, internal corona discharges would occur, causing noticeable errors. Small data variances from run to run were caused by the relative insensitivity of the ammeter in the corona circuit. The smallest scale division of this ammeter was 2 μA and the meter itself had an accuracy no better than ± 2 μA. Other data discrepancies may have been due to humidity variations, misalignment of the corona needle, or power supply irregularities.

Figure 14 is a typical comparison of corona current versus voltage with no airflow for positive and negative needle coronas, using corona unit 1. As shown, a negative needle corona produces much higher corona currents for a given voltage than a positive needle corona, and the breakdown of a negative needle corona greatly exceeds that of the positive needle. However, in subsequent data runs the positive needle corona was used since this polarity produces ions drifting toward the ring of a lower mobility than those produced by a negative needle corona. Thus greater collector currents would be expected with a positive needle corona.

The next chart, Figure 15, shows the results of adding airflow to the positive needle corona. At low test section Mach numbers ($M < 0.3$), the corona current at a given voltage is considerably less and the breakdown potential is slightly higher than that of the no-flow corona. At higher Mach numbers ($M > 0.3$), the corona currents at a given voltage are only slightly less than that of a no-flow corona but the breakdown potentials have dropped considerably. It is believed that this behavior of the corona current --- first decreasing, then increasing as the velocity is increased at a given voltage --- is due to interaction between the velocity and pressure effects on corona efficiency. At low velocities and pressures velocity has a greater effect than pressure, thus causing decreasing current with increasing velocity. After a certain increase in velocity and accompanying decrease in pressure, however, the pressure effect becomes dominant over the velocity effect, causing an increasein corona current with further velocity increase.

The current-voltage-velocity relationship was investigated with a different approach by holding the corona voltage constant and examining how the corona current reacted to changes in air flow rate. The results are shown in Figure 16. It can be seen that addition of flow rate causes an initial drop in corona current at any voltage. The corona current then increases as velocity increases, but tends to remain below the no-flow level. Both the initial drop and gradual increase are more pronounced at high voltages. Data points cross-plotted from Figure 16 to Figure 15 lie on the existing data curves.

Efforts to detect collector current using corona unit 1 at any air flow rate were generally unproductive, and led to the designing of corona unit 2. This unit had the feature of a shorter needle but because of a smaller-radius ring the distance between the needle tip and the ring was the same as that of corona unit 1. Thus the electric field between the needle and the ring would tend to help drive the drifting ions downstream. A main problem encountered was the action of the collector needle as a corona needle when placed close enough to the ring to detect generated current. Any collector current which may have been present was being overshadowed by the backward flowing current of the unwanted corona. This problem was eliminated by placing a set of three International Rectifier Corporation diodes in the collector circuit which prevented any reverse current. Since no collector current was yet detectable, another corona unit, unit 3, was built. This unit had a larger diameter ring which reduced the electric field on the charged ions, enhancing their chances of receiving enough kinetic energy to be blown downstream to the collector. Figure 17 shows the results of this final effort. Since no current was detected with corona units 1 and 2 in the same range of voltages using the diodes to prevent a reverse corona, the currents obtained were reasonably assured to be collector currents rather than reverse current leakage through the diodes. The bars representing data points are due to the fact that these currents were read from a digital ammeter on the last digit of the readout. Thus it was deemed inappropriate to average the values which fluctuated over

the range shown. Collector current increased with increasing voltage, being limited by the breakdown potential of the corona. The optimal collector position was on the corona ring centerline, one inch downstream of the ring plane. Any horizontal or vertical movement from this position caused a decrease in collector current. Changes in air flow rate seemed to make little difference in the amount of collector current, although as can be seen by Figure 17, the amount of current detectable was so minute that changes may have been unreadable due to limitations of the ammeter. The trend of the curve is reasonable in that increased voltage causes increased corona current. As corona current rises, more ions are available for conversion.

VI. RECOMMENDATIONS

As stated earlier, for an EGD system to produce power, the force imparted by the gas flow on the ions of the corona must exceed the attractive force of the corona field. Since variation of the corona voltage is relatively restricted by breakdown, the most apparent improvement would be to increase the rate of energy transfer between the flow particles and the injected ions. On this basis, the following recommendations are made:

a. Investigate further the pressure wake of the cylinder to re-evaluate its effect on the EGD process. The benefits to corona efficiency caused by the decreased pressure of the cylinder wake may be less than the detrimental effects on the conversion process, which is more efficient at higher pressures.

b. Conduct further modified experiments by injecting micron-sized particles (such as dust) into the air flow upstream of the corona unit. Such particle ions have a much lower mobility than air ions and thus should lead to higher conversion efficiencies.

c. Develop a new injection system which would inject micron-sized charged particles into the air flow. (Such a system might use steam as the injection medium. LT(jg) W. T. Ober, USN, has conducted an investigation of a system of this type.[7]) These lower mobility ions would again increase the conversion efficiency.

d. Since ion mobility is reduced by increased pressure, the conversion process would be enhanced if the operating pressure (atmospheric for this investigation) could be increased.

e. Continue efforts to improve data reproductibility by eliminating sources of current leakage and other adverse system variables.

APPENDIX A

Flow Measurements

The experimental facility air flow delivery tube had a square-edged orifice, built to ASME standards,[8] for determination of flow rates. However, the equation for mass flow as determined by this device is awkward and requires an iterative procedure to obtain a value. Since frequent flow rate changes were necessary for this investigation and extremely accurate flow rate determination was not a requirement, it was deemed sufficient to measure flow rate using a pitot-static tube located in the test section. However, the following calculations were made to ascertain how closely the pitot-static and orifice measurements correlated.

The development of the orifice flow rate equation is, according to reference 8:

$$W = 359.1(D_2)^2 Y_1 \propto K\sqrt{\rho_1 h_w} \quad \text{(lb/hr)} \qquad \text{(A-1)}$$

D_2 = orifice diameter, inches

ρ_1 = fluid density at orifice, lb/ft^3

h_w = pressure differential across orifice, inches H_2O

Y_1 = dimensionless expansion factor

K = dimensionless discharge coefficient

$\propto$ = dimensionless area multiplier

$$K = 0.6876 \qquad \text{(Ref. 8, p. 221)} \tag{A-2}$$

ρ_1 may be determined as follows:

$$\rho_1 = MP_1/(10.73)T_1\mu_1 \tag{A-3}$$

T_1 = temperature above orifice, °R

P_1 = absolute pressure above orifice, lb/ft^2

M = 28.96 for air, $\frac{lbm}{lb\text{-mole}}$

$\mu_1 \simeq 1.0$ (Ref. 8, Fig. 138)

Y_1 is obtained from the following formula:

$$Y_1 = 1-(.41 + .35\beta^4)h_w/KP_1 \tag{A-4}$$

β = orifice to pipe diameter ratio

K = 1.4 for air

Y_1, δ, and α are all very close to unity. For D_2 = 2.15 inches, the orifice flow rate equation reduces to:

$$W = 1131\sqrt{\rho_1 h_w} \quad (lb/hr) \tag{A-5}$$

or by the continuity equation:

$$\bar{u} = W/\rho_b A \tag{A-6}$$

A = test channel cross-sectional area

$\bar{u}$ = mass-mean velocity

ρ_b = fluid density in test channel

The equation for flow determination by the pitot tube is derived from Bernoulli's equation:

$$p_a + \rho_a U_a^2/2g = p_b + \rho_b U_b^2/2g \qquad \text{(A-7)}$$

but $U_a = 0$, $\rho_a = \rho_b$, giving after rearrangement:

$$U_\infty = \sqrt{2g\Delta P/\rho_b} \quad \text{(ft/sec)} \qquad \text{(A-8)}$$

$g = 32.2$ ft/sec^2

ΔP = pitot tube pressure differential, cm H_2O.

However, the orifice equation gives mass-mean flow rate while the pitot tube indicates freestream velocity. Therefore, the pitot tube value is corrected according to Reference 9, page 536. For a 1/7-power velocity distribution, in the boundary layer,

(u/U_∞) average = .875.

Therefore, the mass-mean velocity can be computed by the following formula:

$$\bar{u} = [A' \times u] + [(1-A') \times U_\infty] \qquad \text{(A-9)}$$

u = average velocity in the boundary layer

U_∞ = freestream velocity

A' = percent of cross-sectional area within the boundary layer.

Assuming a boundary layer thickness of 0.1 inch, A-9 reduces to:

$$\bar{u} = .28u + .72U_\infty \qquad \text{(A-10)}$$

or

$$\bar{u} = .965U_\infty \qquad \text{(A-11)}$$

The following data is reduced for comparison:

Orifice	Pitot Tube
$t_1 = 69°F$	$t_2 = 68°F$
$h_w = 26.1$ cm H_2O	$\Delta P = 46.3$ cm H_2O
$P_1 = 86.6$ cm H_2O	$P_2 = 70.0$ cm H_2O
b = 30.06 in Hg	b = 30.06 in Hg
$\rho_1 = .0819$ [by (A-3)]	$\rho_b = .0806$ [by (A-3)]
	$U_\infty = 276$ ft/sec [by (A-8)]
$\bar{u} = 280$ ft/sec [by (A-6)]	$\bar{u} = 266$ ft/sec [by (A-11)]

Thus flow rate determination using the pitot-static tube yields values approximately 5% in error on the low side. Assuming constant density for air, the following formula, which includes a factor to correct for this error, was used to compute flow velocities:

$$\bar{u} = 40.95\sqrt{\Delta P} \quad \text{(ft/sec)}$$

As before, ΔP is the pitot-static tube pressure differential in centimeters of water.

APPENDIX B

Flow Determination Instrumentation

Before choosing the means of determining the flow properties of the test channel, four different devices were considered: the hot-wire anemometer, thermistor, conductivity probe, and pitot-static tube. The thermistor and conductivity probes are devices which measure temperature and temperature fluctuations. The thermal sensitivity of the thermistor is about twice that of the conductivity probe (-4%/°C versus -2%/°C) but has a slower frequency response. However, both the thermistor and the conductivity probe are insensitive to velocity fluctuations.[10] Inasmuch as the flow properties which were under investigation were velocity and velocity fluctuations (turbulence), the thermistor and conductivity probe were immediately eliminated as useful.

Thus it was decided to use the hot-wire anemometer which gives both the relative velocity (generally the output indicator is adjusted to maximum scale for a specific local velocity) and, in conjunction with a RMS voltmeter, velocity fluctuations. This device utilizes King's Law which gives the rate of heat loss from an electrically heated fine wire exposed to a flow:

$$q = (A + B\sqrt{U})\ (T_w - T_f)$$ where

q = rate of heat loss

T_w = wire temperature

T_f = flow field temperature

U = velocity normal to the wire

A and B are constants dependent on geometrical factors and fluid property values. A hot-wire system may be operated in one of two modes: constant current or constant temperature. The constant temperature mode has a frequency response several orders higher than the constant current mode and thus has better response characteristics. In this mode a feedback amplifier is employed which senses the wire resistance and adjusts the wire heating current to maintain a constant wire temperature. Changes in flow velocity over the wire cause heating loss rate changes which are sensed by the amplifier as resistance changes. The hot-wire anemometer system used was a Security Associates Constant Temperature Hot-Wire Anemometer which utilizes a built-in analogue computer circuit to linearize the output.

In addition, a pitot-static tube was used to measure the flow mean velocity.

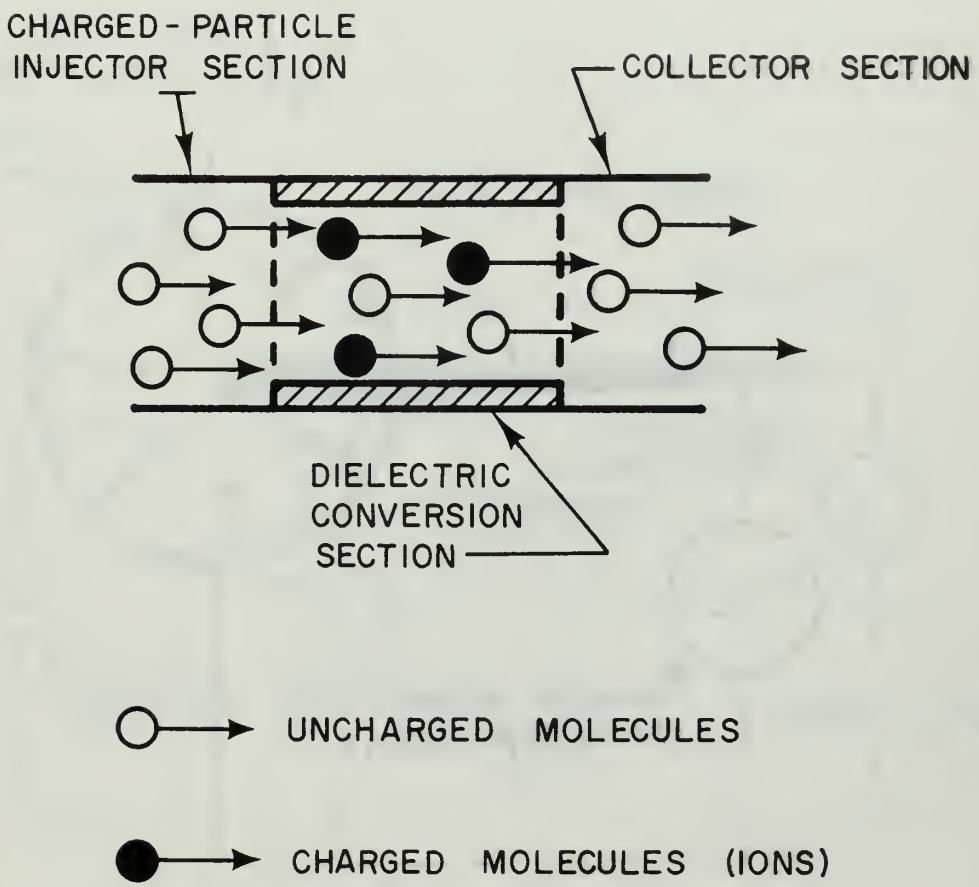

FIGURE I. EGD GENERATOR SCHEMATIC

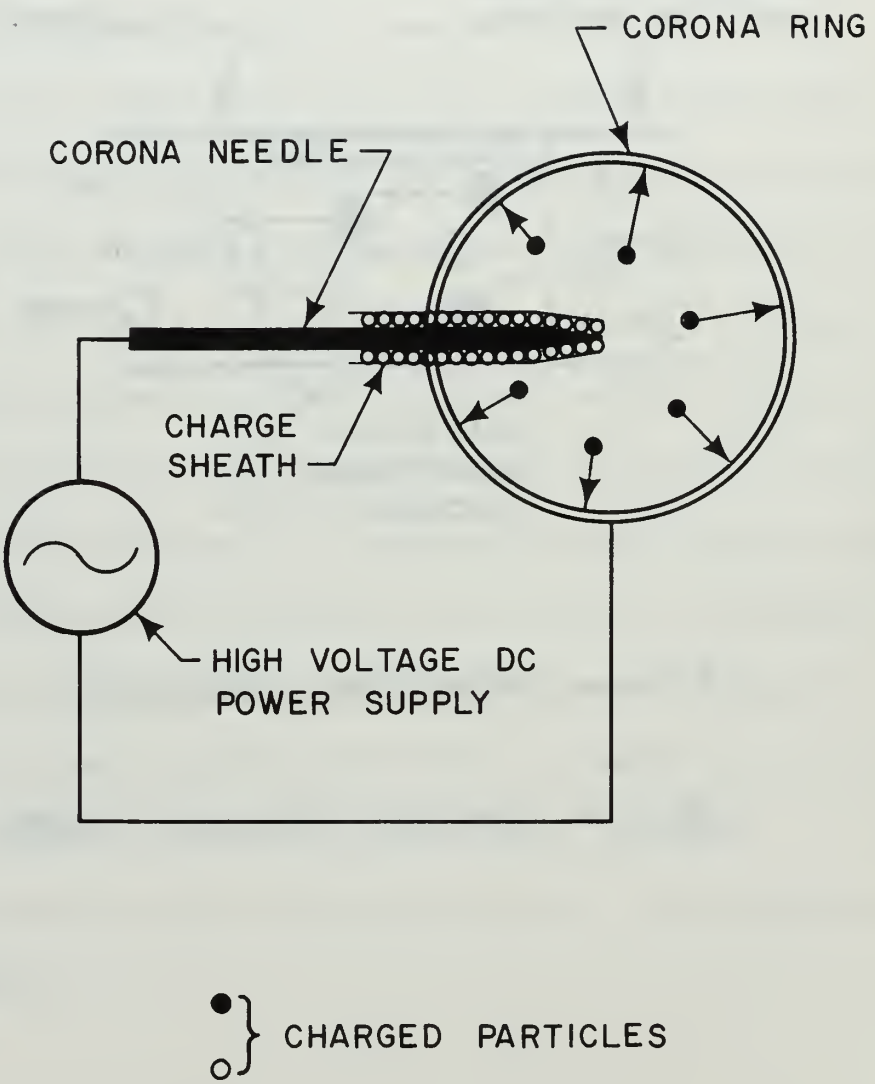

FIGURE 2. CORONA DISCHARGE PRINCIPLE

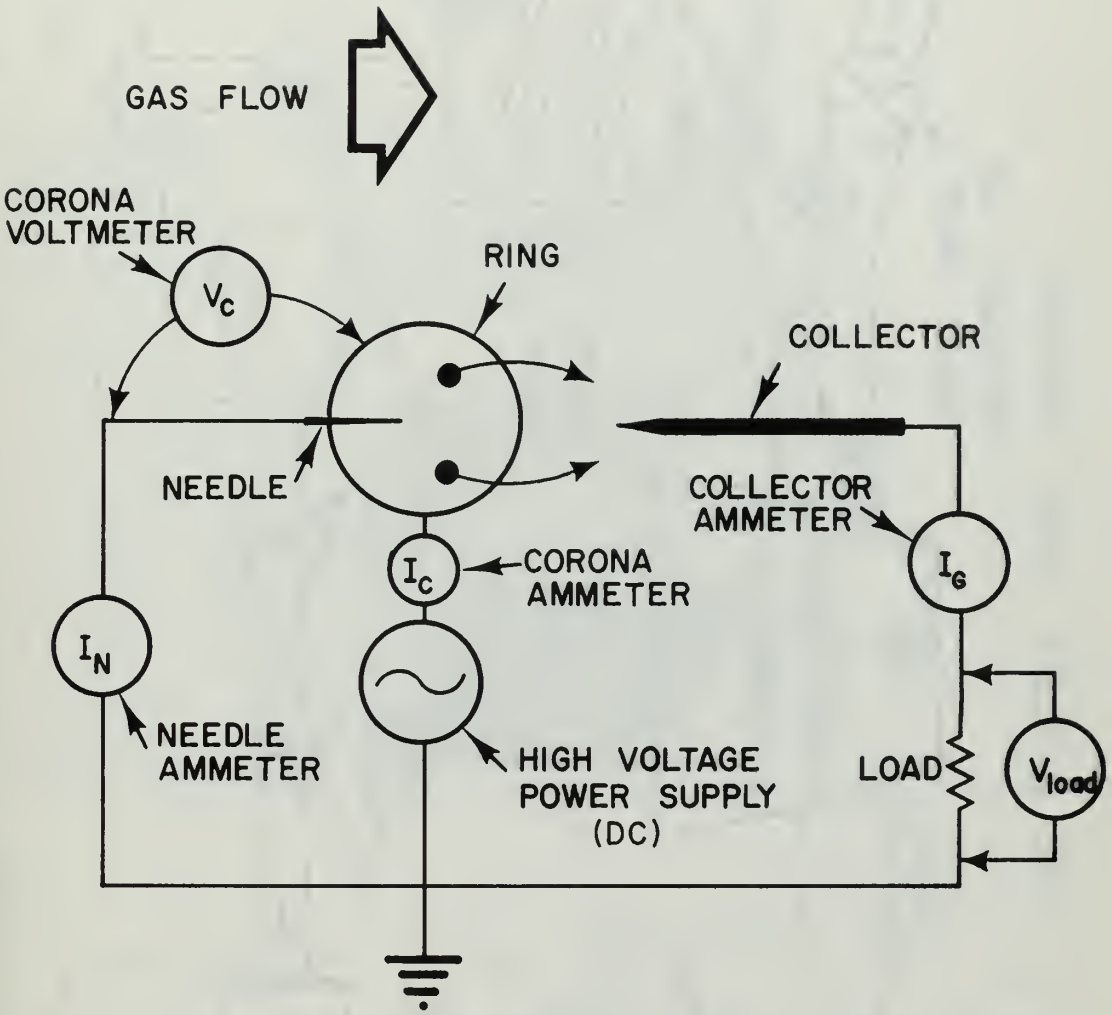

FIGURE 3. EGD SYSTEM WIRING CIRCUIT

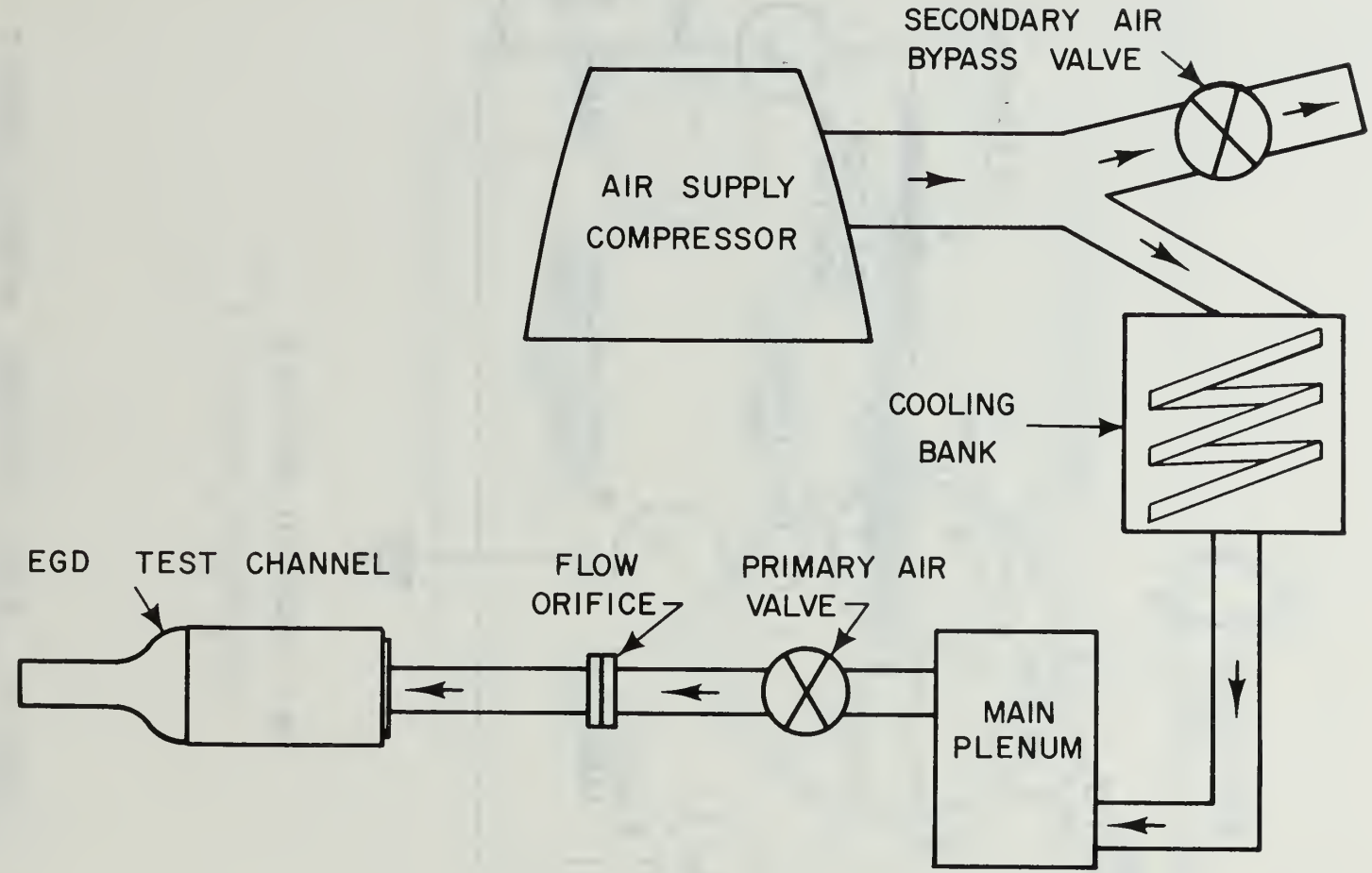

FIGURE 4. EGD SYSTEM SCHEMATIC

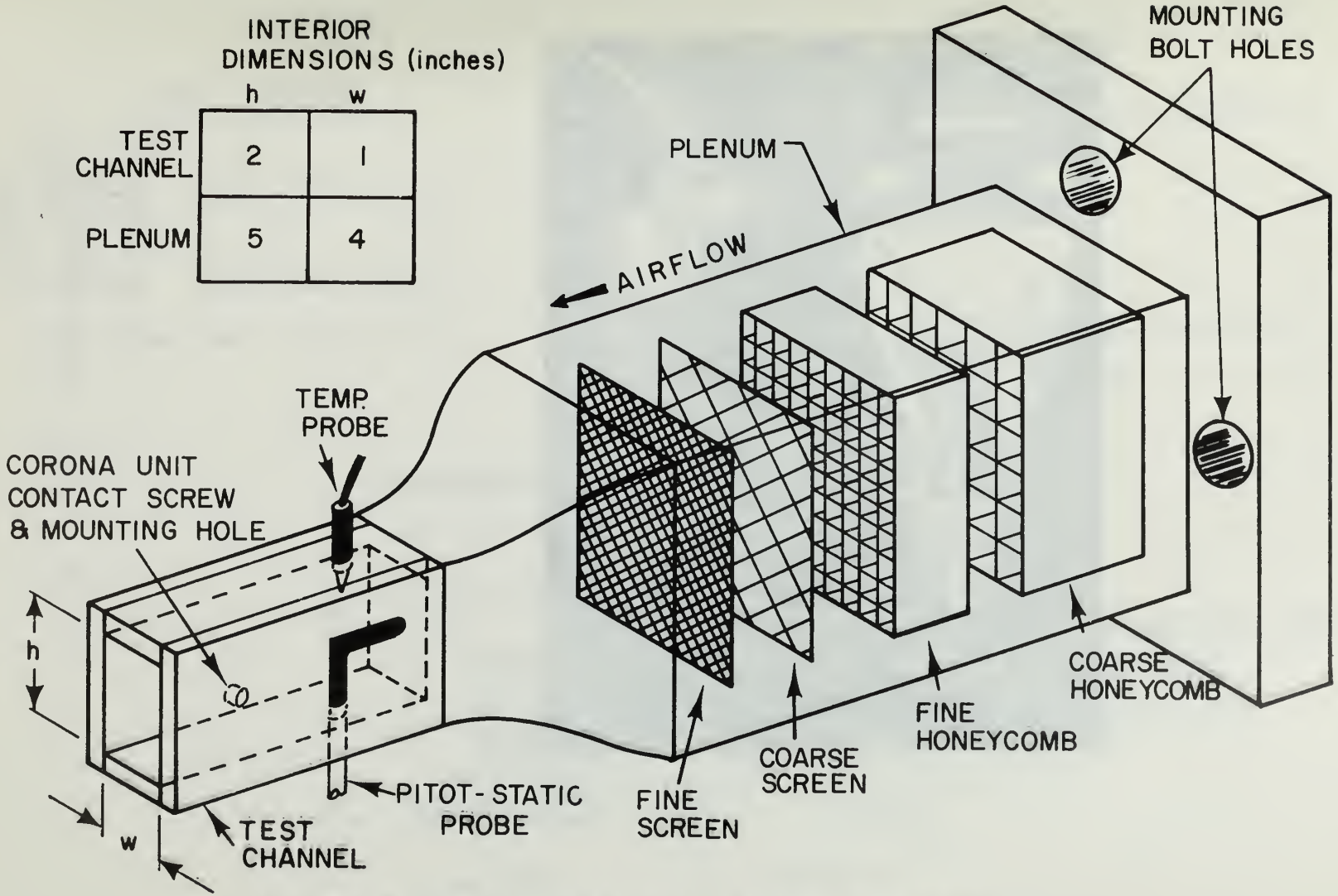

FIGURE 5. EGD SYSTEM FLOW CHANNEL

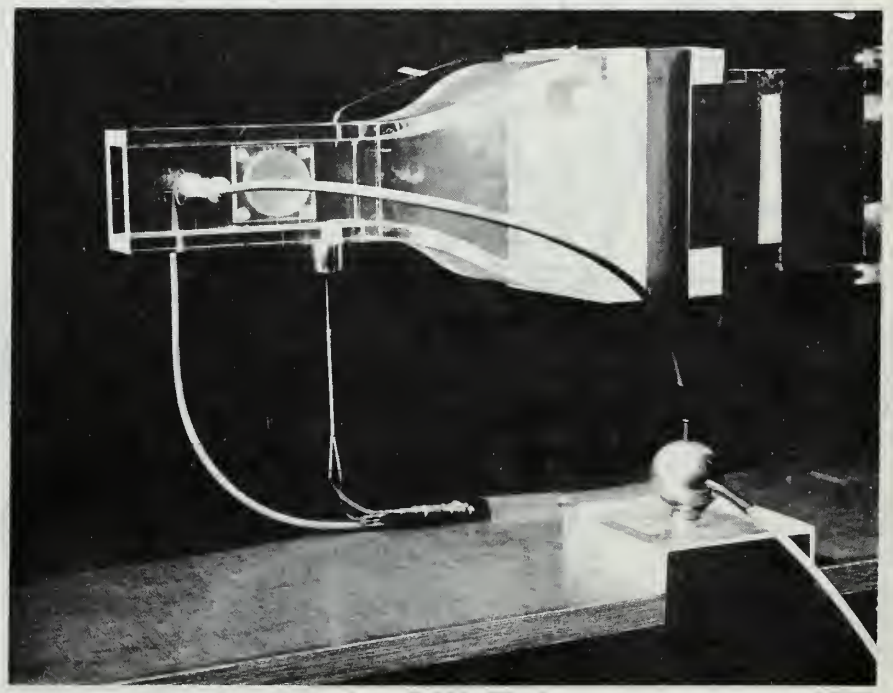

FIGURE 6 ECD SYSTEM FLOW CHANNEL

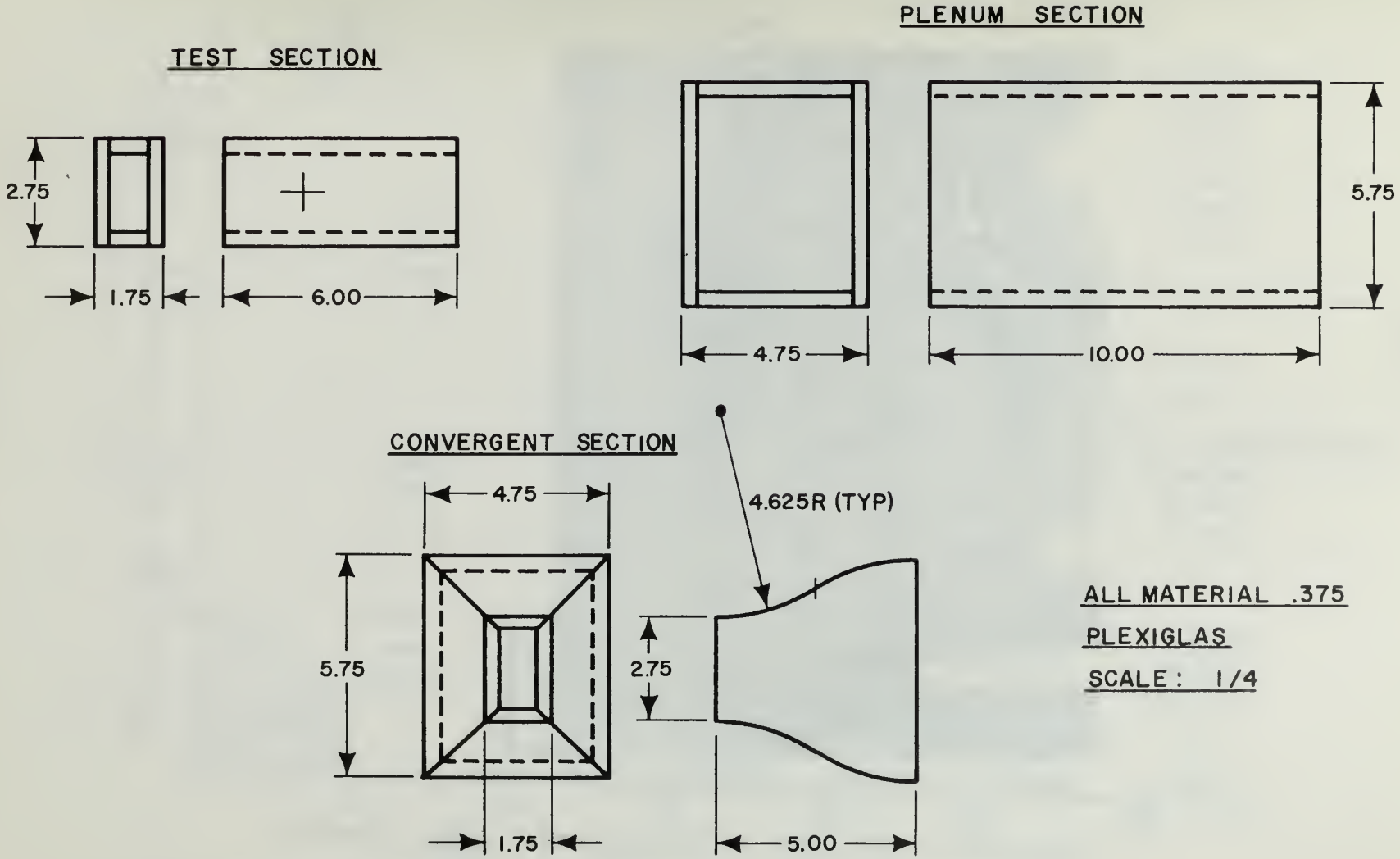

FIGURE 7. EGD SYSTEM FLOW CHANNEL

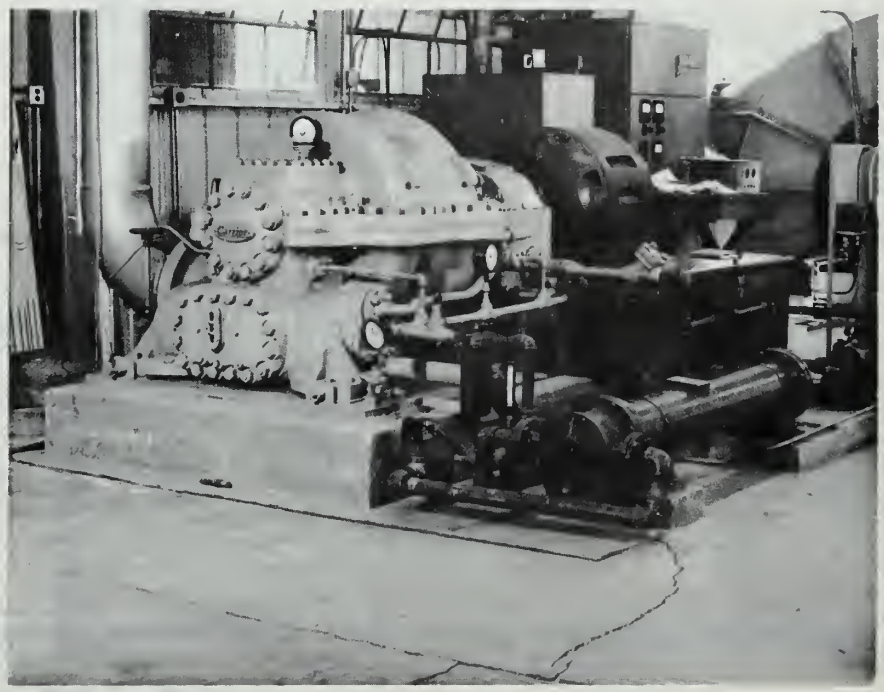

FIGURE 8. COMPRESSOR

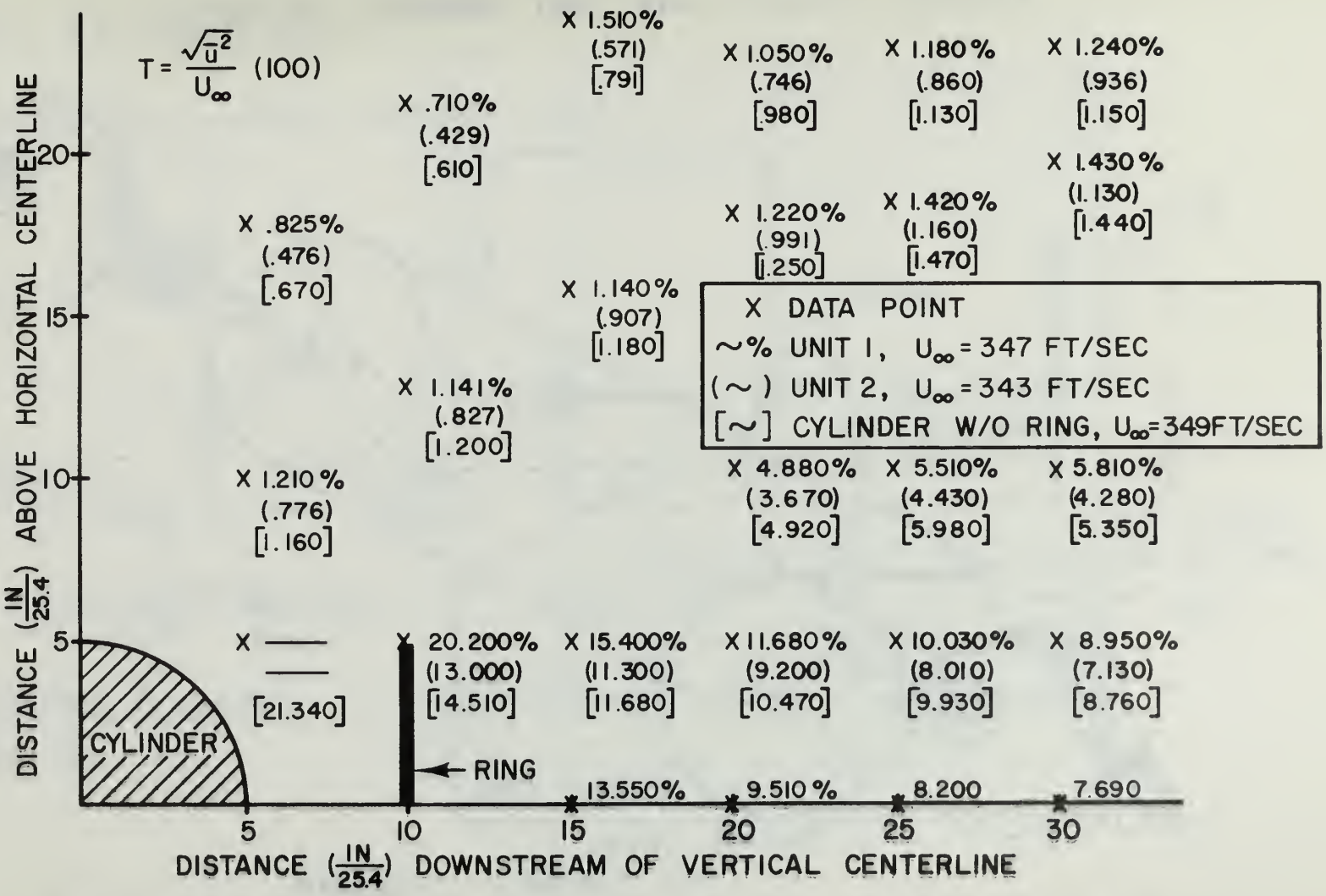

FIGURE 9. TURBULENCE LEVELS AT VARIOUS WAKE POSITIONS

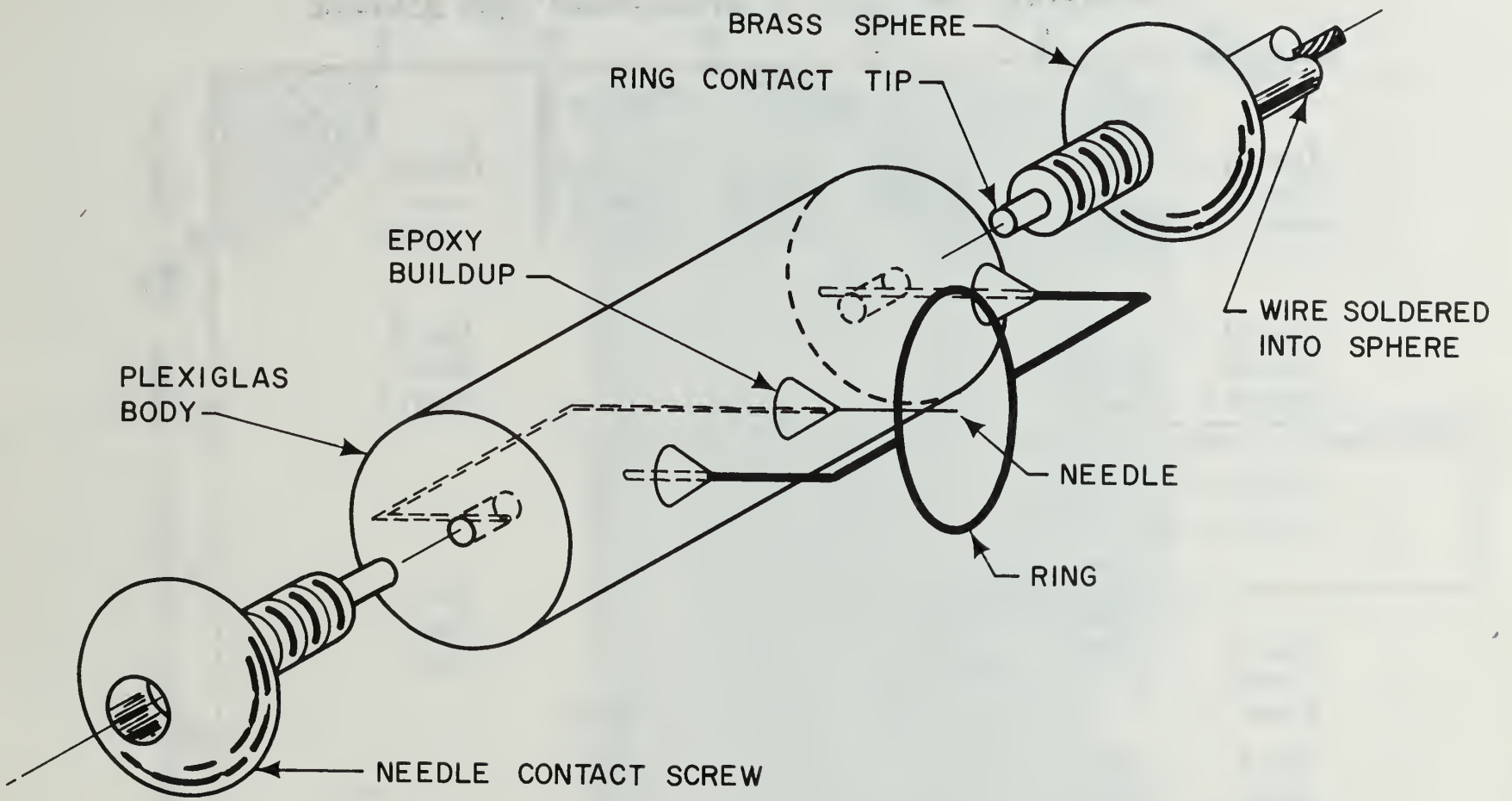

FIGURE 10. CORONA UNIT AND CONTACT SCREWS

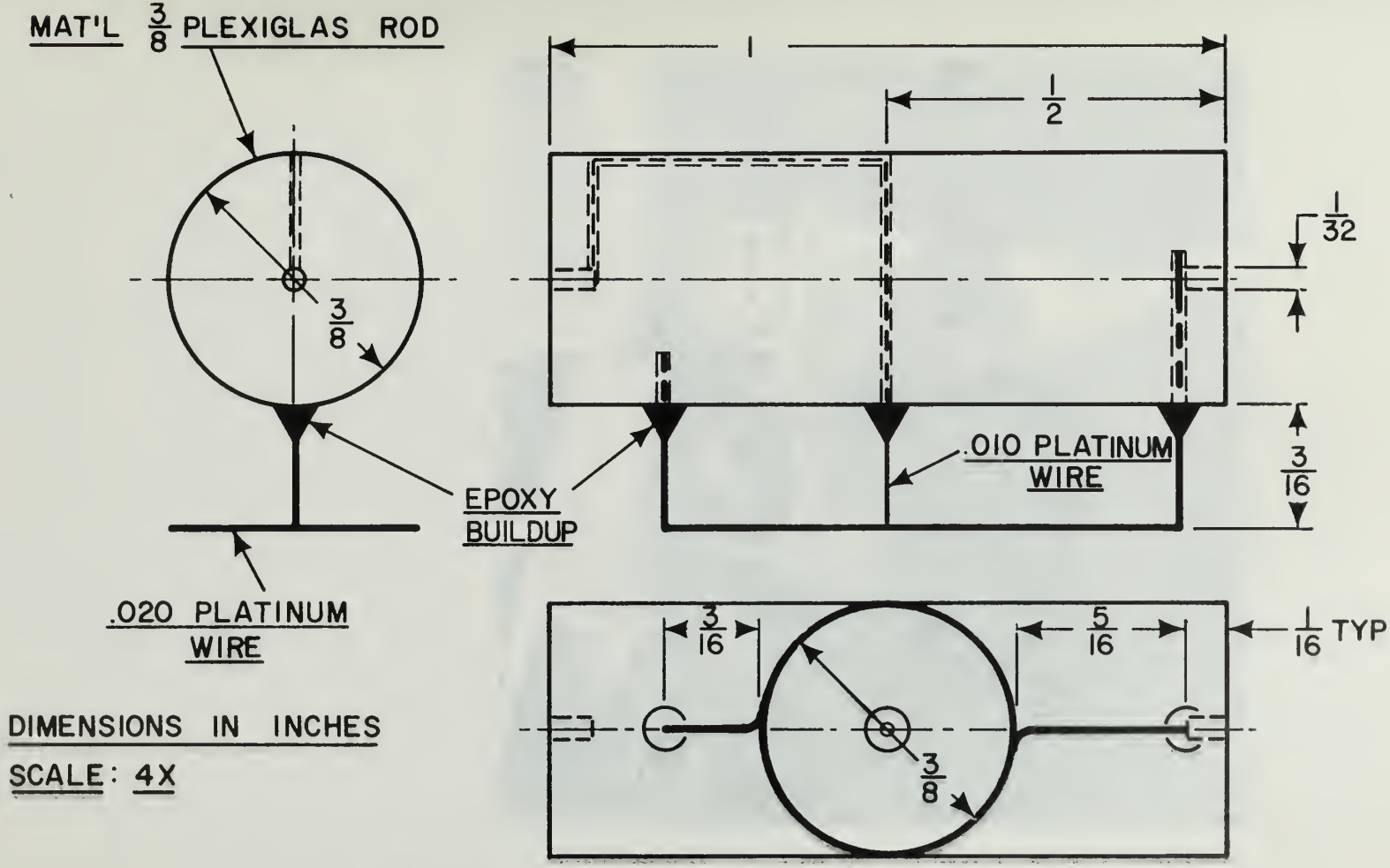

FIGURE II. CORONA UNIT

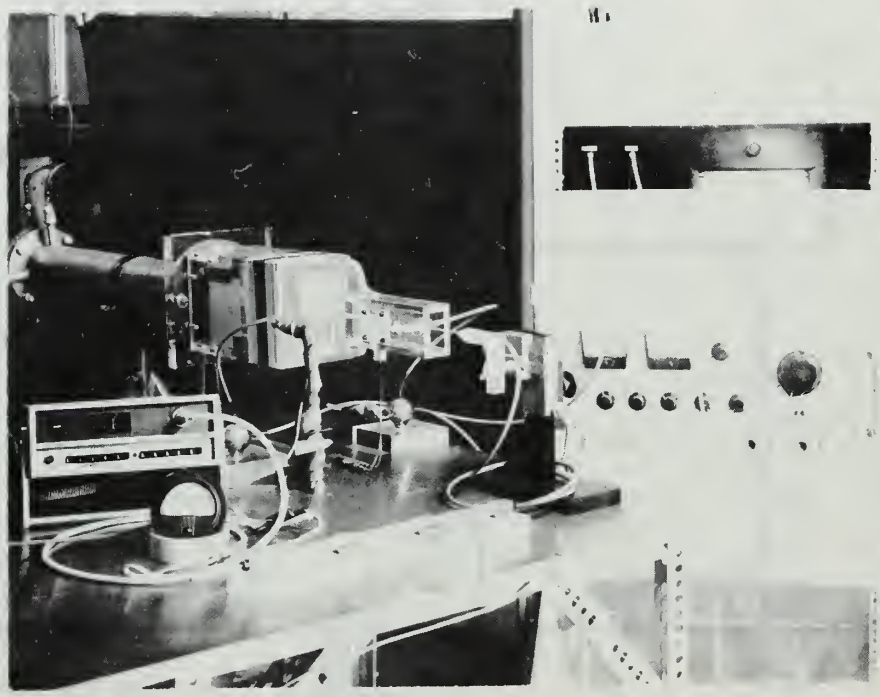

FIGURE 16. INSTRUMENTATION

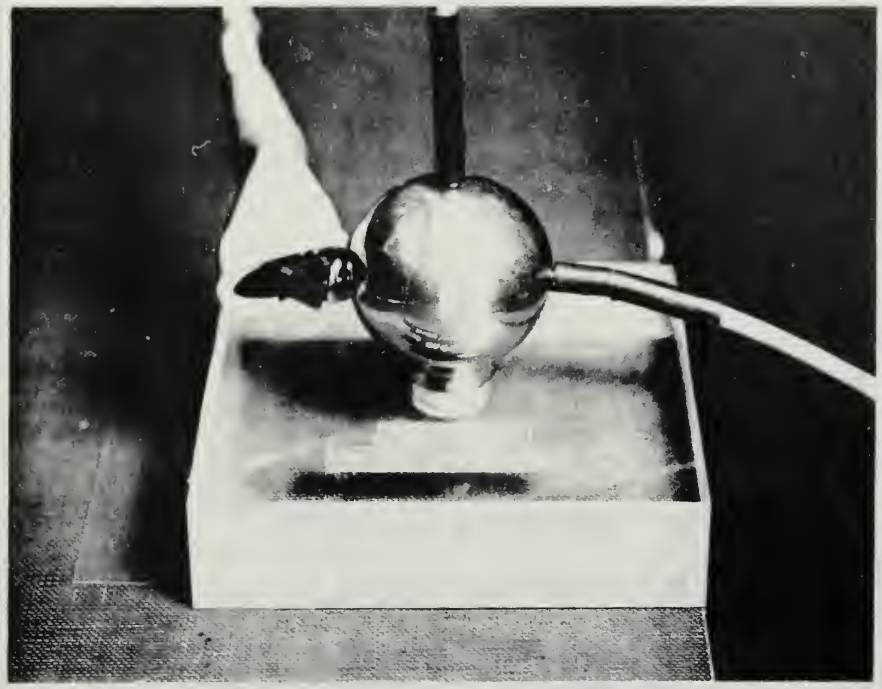

FIGURE 7.1. CONTROL SPHERE

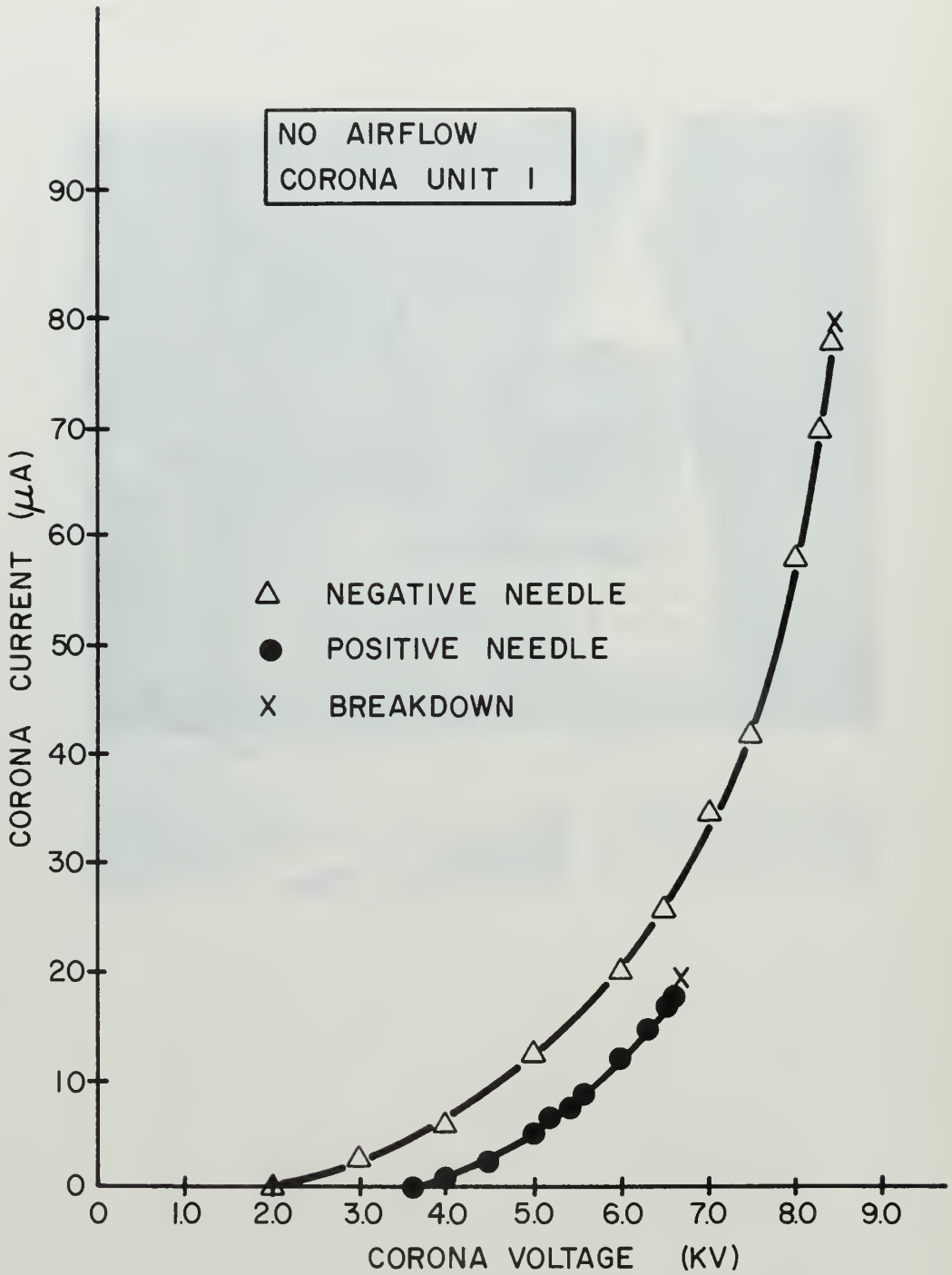

FIGURE 14. CORONA CURRENT VS VOLTAGE

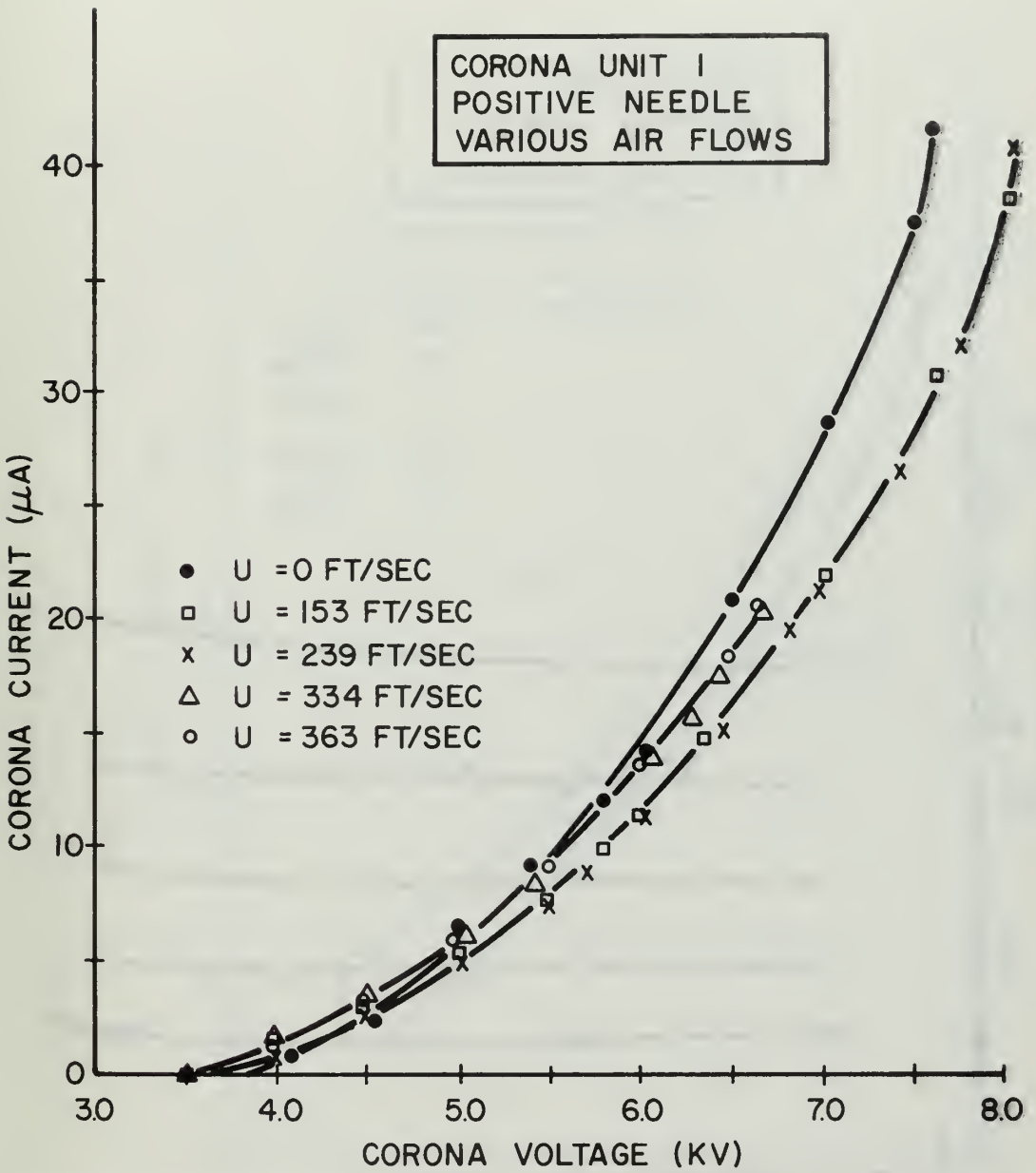

FIGURE 15. CORONA CURRENT VS VOLTAGE

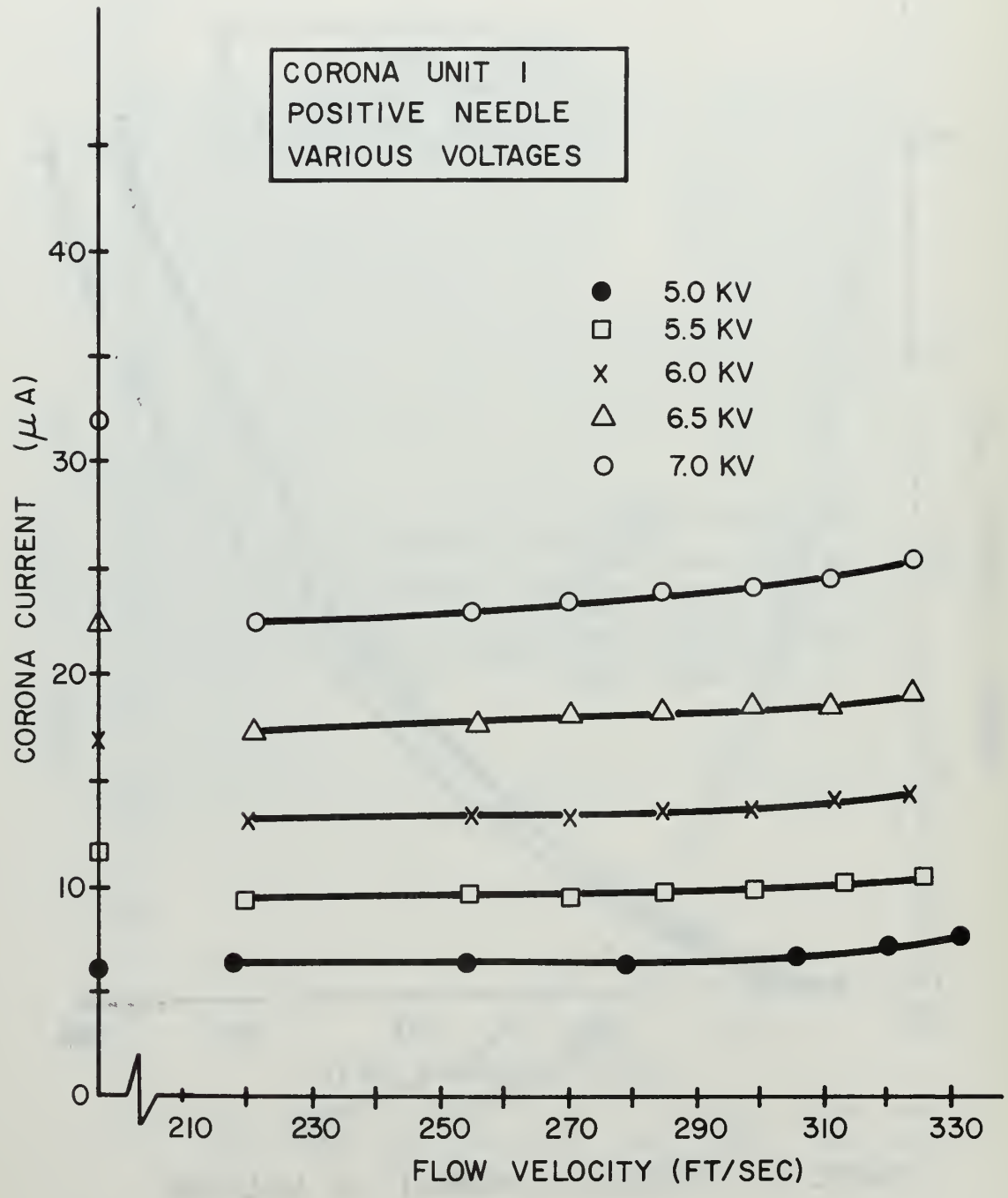

FIGURE 16. CORONA CURRENT VS FLOW RATE

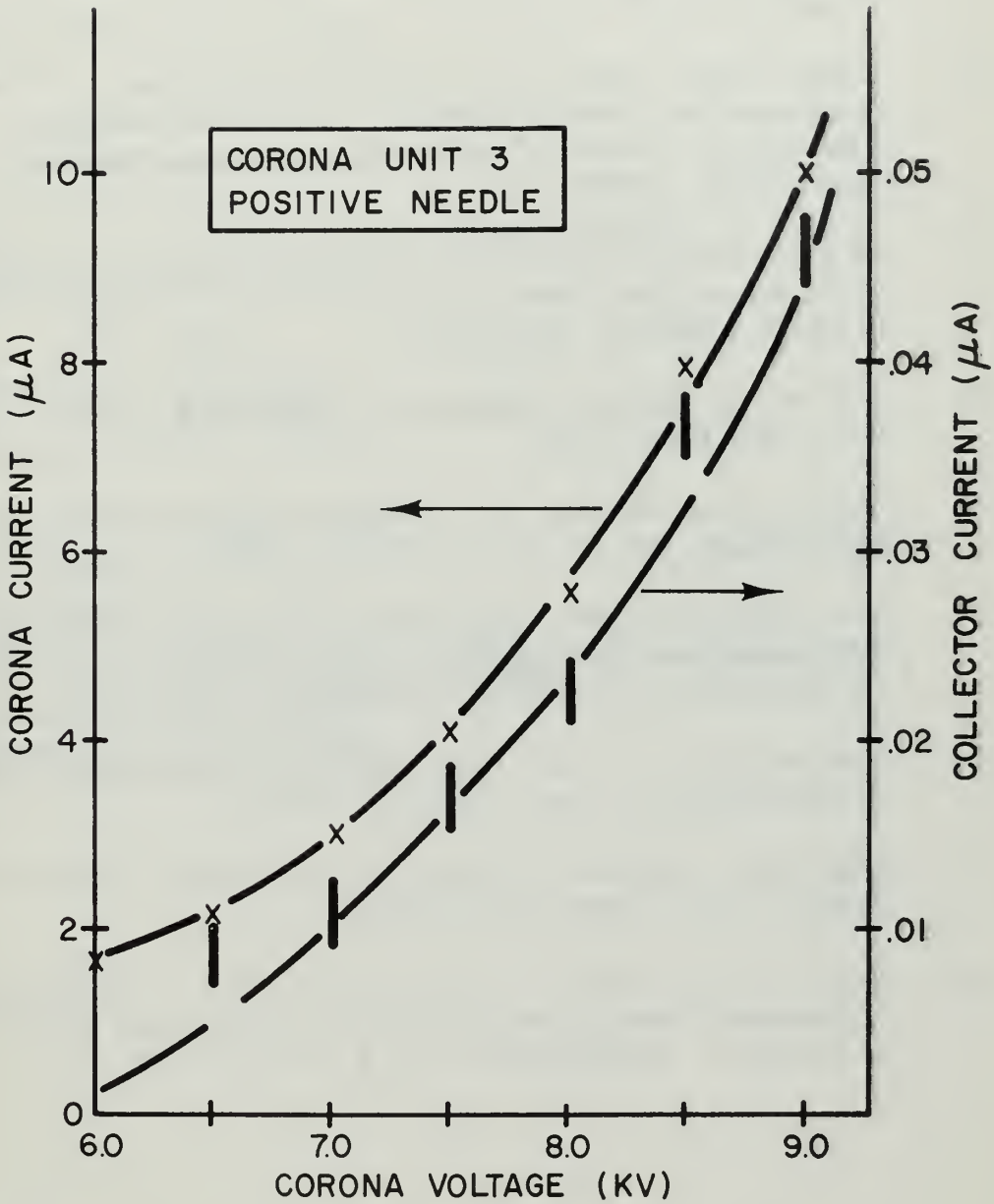

FIGURE 17. CORONA AND COLLECTOR CURRENT VS VOLTAGE

BIBLIOGRAPHY

1. Bennett, W. E. "The Generation of Direct Current at High Potentials." Research Applied in Industry, Vol. 12, No. 12, December 1959, England.

2. Smith, J. M. Electrohydrodynamic Power Generation--- Experimental Studies. General Electric Space Sciences Laboratory Report, March 1962.

3. Decaire, Capt. John A. and Wifall, Capt. James R. "Charge Generation by Corona Discharge in Electrofluiddynamic Conversion Processes." Advances in Energy Conversion Engineering. ASME, 1967.

4. Charged Particle Power Generation and Propulsion. Maremont Corporation, Final Report on Contract NOw 64-0594-f, Bureau of Naval Weapons, Washington, D. C., July, 1966.

5. Cobine, J. Gaseous Conductors. McGraw-Hill Book Company, Inc., New York, 1969.

6. Marks, A. and Barreto, E. "Charged Aerosol Energy Converter." AIAA Journal, Vol. 2, No. 45, January 1964.

7. Ober, LT(jg) William. Ion Injector for Single and Two-phase Electrogasdynamic Generators. Master Thesis, Naval Post-graduate School, Monterey, California. June, 1969.

8. Stearnes, R. F., et al. Flow Measurement with Orifice Meters. Van Nostrand Co., Inc., New York, 1960.

9. Schlichting, Hermann. Boundary Layer Theory. McGraw-Hill Book Co., Inc., New York, 1960.

10. Gibson, C. H., Chen, C. C., and Lin, S. C. "Measurements of Turbulent Velocity and Temperature Fluctuations in the Wake of a Sphere." AIAA Journal, Vol. 6, No. 4, 1968.

INITIAL DISTRIBUTION LIST

		No. Copies
1.	Defense Documentation Center Cameron Station Alexandria, Virginia 22314	20
2.	Library Naval Postgraduate School Monterey, California 93940	2
3.	Commander Naval Air Systems Command Department of the Navy Attention: Mr. Milton Knight, Code AIR-340C Washington, D. C. 20360	1
4.	Professor O. Biblarz Department of Aeronautics Naval Postgraduate School Monterey, California 93940	4
5.	LT(jg) D. W. Wallace, USN 2207 Jameson St., S.E. Washington, D. C. 20031	1
6.	Chairman, Department of Aeronautics Naval Postgraduate School Monterey, California 93940	1

Security Classification

DOCUMENT CONTROL DATA - R & D

(Security classification of title, body of abstract and indexing annotation must be entered when the overall report is classified)

1. ORIGINATING ACTIVITY (Corporate author)	2a. REPORT SECURITY CLASSIFICATION
Naval Postgraduate School Monterey, California 93940	Unclassified
	2b. GROUP

3. REPORT TITLE

Molecular-ion Electrogasdynamic Flow Channel

4. DESCRIPTIVE NOTES (Type of report and inclusive dates)

Master's Thesis; June 1969

5. AUTHOR(S) (First name, middle initial, last name)

David William Wallace

6. REPORT DATE	7a. TOTAL NO. OF PAGES	7b. NO. OF REFS
June 1969	52	10

8a. CONTRACT OR GRANT NO.	9a. ORIGINATOR'S REPORT NUMBER(S)
b. PROJECT NO.	
c.	9b. OTHER REPORT NO(S) (Any other numbers that may be assigned this report)
d.	

10. DISTRIBUTION STATEMENT

Distribution of this document is unlimited

11. SUPPLEMENTARY NOTES	12. SPONSORING MILITARY ACTIVITY
	Naval Postgraduate School Monterey, California 93940

13. ABSTRACT

This investigation evaluates the operating characteristics of an EGD (electrogasdynamic) generator system which utilizes air both as the carrier fluid and as the source of injected ions. The design and construction of a flow channel and a corona ion injector are discussed, the performance of the ion injector is examined, and the results of attempts to obtain work by EGD energy conversion are presented. The experimental results presented and discussed are in reasonable agreement with expectations. The high mobility of molecular ions inhibits the conversion process and only 0.5% of the ions were removed from the corona by the air flow. Suggestions for improvements on the present system and the design of an advanced system are made.

DD FORM 1 NOV 65 1473 (PAGE 1)

S/N 0101-807-6811

Security Classification

A-31408

14 KEY WORDS	LINK A		LINK B		LINK C	
	ROLE	WT	ROLE	WT	ROLE	WT
electrogasdynamic corona discharge ion injector energy conversion						